



Recent Results on Charm from Fermilab Experiment E-687*

The E-687 Collaboration

presented by

D. Buchholz
*Northwestern University
Evanston, Illinois 60208*

S. Gourlay
*Fermi National Accelerator Laboratory
P.O. Box 500
Batavia, Illinois 60510*

L. Moroni
*Dip. di Fisica dell'Universita' and INFN
Milan, Italy*

S. P. Ratti
*Dip. di Fisica Nucleare dell'Universita' and INFN
Pavia, Italy*

W. D. Shephard
*University of Notre Dame
Notre Dame, Indiana 46556*

December 1990

* To be published in the proceedings of the XXVth International Conference on High Energy Physics, Kent Ridge, Singapore, August 2-8, 1990.



RECENT RESULTS ON CHARM FROM FERMILAB EXPERIMENT E687

P.L. Frabetti

Dip. di Fisica dell'Universita' and INFN - Bologna, I-40126 Bologna, Italy

C.W. Bogart, H.W.K. Cheung, P. Coteus, S. Culy, J.P. Cumalat, D. Kaplan
University of Colorado, Boulder, CO 80309, USA

J.N. Butler, F. Davenport, I. Gaines, P.H. Garbincius, S. Gourlay, D.J. Harding, P. Kasper, A. Kreymer,
P. Lebrun, H. Mendez
Fermilab, Batavia, IL 60510, USA

S. Bianco, M. Enorini, F.L. Fabbri, A. Spallone, A. Zallo
Laboratori Nazionali di Frascati dell'INFN, I-00044 Frascati, Italy

R. Culbertson, M. Diesburg, G. Jaross, K. Lingel, P.D. Sheldon, J.R. Wilson, J. Wiss
University of Illinois at Urbana-Champaign, Urbana, IL 61801, USA

G. Alimonti, G. Bellini, M. Di Corato, M. Giammarchi, P. Inzani, S. Malvezzi, P.F. Manfredi, D. Menasce,
L. Moroni, D. Pedrini, L. Perasso, A. Sala, S. Sala, D. Torretta, M. Vittone
Dip. di Fisica dell'Universita' and INFN - Milano, I-20133 Milan, Italy

D. Buchholz, B. Gobbi, S. Park, R. Yoshida
Northwestern University, Evanston, IL 60208, USA

J.M. Bishop, J.K. Busenitz, N.M. Cason, J.D. Cunningham, R.W. Gardner, C.J. Kennedy, E.J. Mannel,
R.J. Mountain, D.L. Puseljic, R.C. Ruchti, W.D. Shephard, M.E. Zanabria
University of Notre Dame, Notre Dame, IN 46556, USA

C. Castoldi, S.P. Ratti
Dip. di Fisica Nucleare dell'Universita' and INFN - Pavia, I-27100 Pavia, Italy

A. Lopez
University of Puerto Rico at Mayaguez, Puerto Rico

Presented for Fermilab E687 Collaboration by D. Buchholz, S. Gourlay, L. Moroni, S.P. Ratti, W.D. Shephard

ABSTRACT

About 10^4 charm decays have been reconstructed from first-run data of Fermilab experiment E687 using the Fermilab Wide-Band Photon Spectrometer with the world's highest energy photon beam. The success of techniques for isolating and reconstructing charm event samples based on two complementary vertexing strategies is illustrated. Preliminary results are presented. These include lifetime values of $(0.50 \pm 0.06 \pm 0.03)$ ps for the D_s^+ , and $(0.20 \pm 0.03 \pm 0.03)$ ps for the Λ_c^+ . Preliminary values for the D^+ and D^0 lifetimes are consistent with currently accepted world averages. Signals for the Cabibbo-suppressed decays $D^0 \rightarrow \pi^+\pi^-\pi^+\pi^-$, $D^+ \rightarrow K^+K^-\pi^+$, and $D^+ \rightarrow \phi\pi^+$ are shown; for $B(D^0 \rightarrow \pi^+\pi^-\pi^+\pi^-)/B(D^0 \rightarrow K^-\pi^+\pi^+\pi^-)$ our preliminary value is $0.10 \pm 0.02 \pm 0.02$. Preliminary values for ratios $B(D^0 \rightarrow \bar{K}^0 K^+ K^-)/B(D^0 \rightarrow \bar{K}^0 \pi^+ \pi^-)$ and $B(D^0 \rightarrow \bar{K}^0 \phi)/B(D^0 \rightarrow \bar{K}^0 \pi^+ \pi^-)$ are 0.20 ± 0.06 and 0.16 ± 0.06 . (statistical errors only). Preliminary results are given for cross sections of $D^{*\pm}$ and D^\pm photoproduction on a Be target over the photon energy range from 100 to 350 GeV, for the p_T dependence of D^{*-} and D^+ photoproduction and for the ratios D^{*-}/D^{*+} and D^{*-}/D^+ . The energy dependence of the total open charm photoproduction cross section is compared with model predictions for photon energies up to 350 GeV.

INTRODUCTION AND SPECTROMETER

Even though colliding e^+e^- beams provide a clean way of producing charm particles, photoproduction experiments afford several advantages; absolute production rates are orders of magnitude higher in photon beams, all portions of the charmed quark invariant mass spectrum can be observed simultaneously, and lifetimes can be measured more easily. Recent advances in detectors, especially silicon microstrips, have enabled photoproduction experiments to reduce backgrounds to a point where quite large charm samples can be obtained. Fermilab experiment E687 uses the world's highest energy photon beam and a new highly-efficient, large-acceptance, high-rate multiparticle spectrometer to study production and decay of charm particles. Summarized here are preliminary results from the first run in which about 45 million hadronic-event γ Be triggers were recorded. Unless otherwise stated, charge conjugate states are included with specific charm decay modes. Samples from the first run include about 10^1 reconstructed charm decays isolated and reconstructed with the use of two complementary vertexing strategies. More details can be found in 5 papers submitted to this conference [1][2][3][4][5]. The second run of E687 will provide more than 5 times more data for future analysis.

The two magnet spectrometer includes a vertex detector and 5 multiwire proportional chambers of 4 planes each for charged-particle tracking. The vertex detector consists of 4 sets of 3 views each of Si microstrip planes with pitch ranging from $25\mu\text{m}$ to $100\mu\text{m}$ for a total of about 8,000 channels. Its resolution, expressed as the predicted transverse error at the mean interaction point in the target for an infinite momentum track traversing the high-resolution region of the planes, is $\sigma_{x,y} \approx 9\mu\text{m}$ corresponding to $\sigma_\tau \approx 0.03\text{ps}$. Neutral vees are reconstructed over a 10m decay length. Charged particles are identified over a wide momentum range by 3 multicell Čerenkov detectors with pion thresholds of 4.4, 6.7, and 17 GeV/c which provide unique identification of kaons from 17 to 44 GeV/c and protons from 17 to 44 GeV/c and 61 to 116 GeV/c and identification of "heavy" (K/p ambiguous) particles from 4.4 to 17 and 44 to 61 GeV/c. Electrons and photons are measured in 3 electromagnetic calorimeters, hadron energy is measured in 2 hadron calorimeters, and muons are identified by 2 sets of detectors. See Refs. [2] and [6] for more details.

The bremsstrahlung photon beam was obtained from 350 GeV/c electrons with a 13% momentum

spread striking a 27% radiator. Photon energy was measured by recoil electron detection. A Be target was used for most of the run. Data were taken with a trigger demanding at least two tracks in the spectrometer, both required to be outside the e^+e^- pair production region, and an energy deposit larger than a specified minimum (typically about 35 GeV) in the hadron calorimeter. The average photon energy for hadronic triggers was 221 GeV.

VERTEXING AND CHARM SELECTION

Two different basic approaches have been used in the selection of charm events:

- a stand-alone algorithm making use only of geometrical track information to construct the complete vertex topology of the event;
- a candidate-driven algorithm selecting a particular decay channel and using the candidate vertex and momentum as a seed to find the primary vertex.

The first algorithm selects events on the basis of evidence for reconstructed secondary vertices; the second simply tests a hypothesis. As a result, the efficiency of the first method tends to be smaller, especially at short lifetimes, but the resultant sample is very clean. The efficiency of the second method depends less, in principle, on proper time, but there is more background at short lifetimes normally requiring a cut. Both techniques rely heavily on the resolution of the microstrip detector.

After event reconstruction, various subsamples were selected in accordance with the two vertexing algorithms described above. The results are illustrated for $D^+ \rightarrow K^-\pi^+\pi^+$ decays. Similar results for $D^0 \rightarrow K^-\pi^+$ and $D^0 \rightarrow K^-\pi^+\pi^+\pi^-$ decays are shown in Ref. [3]. Fig. 1 show the effects of different cuts (see caption) on the original sample using the stand-alone vertexing method. Plot 1f) shows that, even without Čerenkov identification, the stand-alone algorithm can extract a D^+ signal; Čerenkov information provides significant further improvements in the signal-to-noise ratio.

With the candidate-driven algorithm, combinations of tracks satisfying requirements on track reconstruction and linking between MWPC's and microstrips, net charge, Čerenkov identification, etc. consistent with the charm decay hypothesis under study are first selected. A secondary vertex formed from the selected tracks is required to meet appropriate criteria. A seed track is constructed from the momentum vectors of the charm candidate daughter tracks. Other tracks intersecting the seed track are used to make a primary vertex which must satisfy additional criteria including cuts on its location.

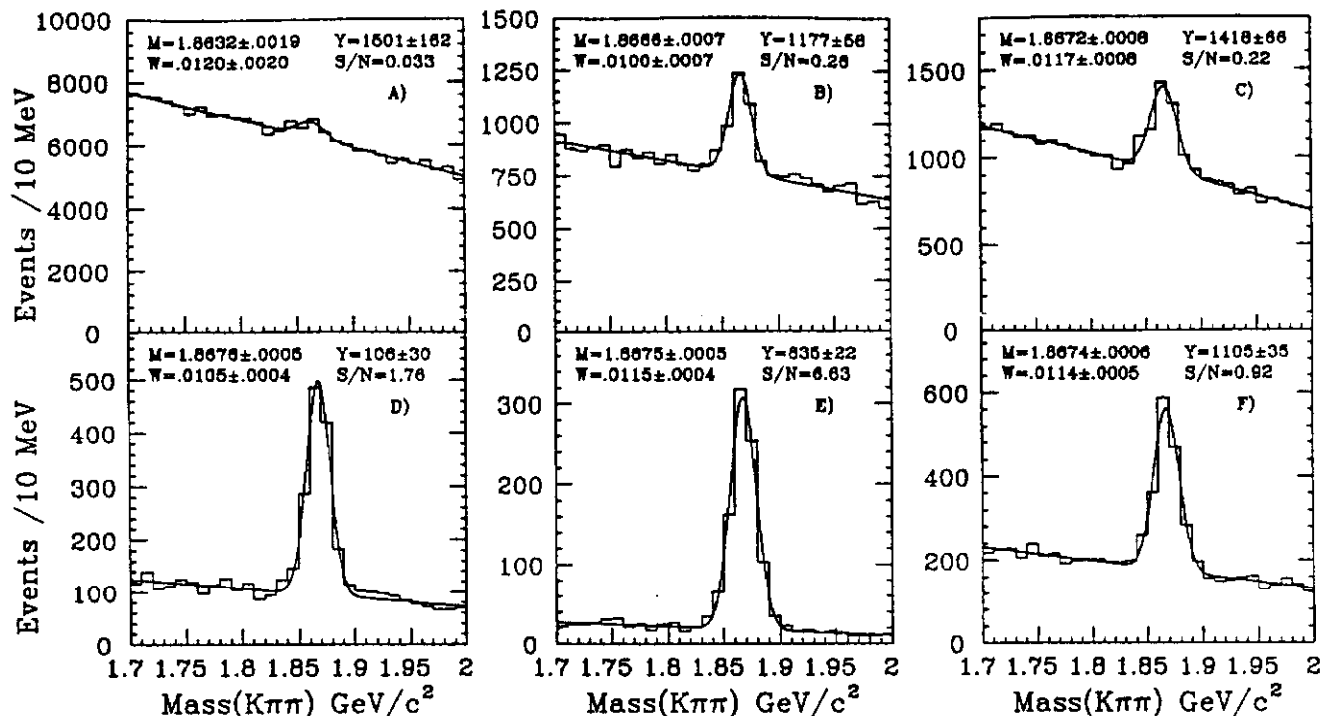


Fig. 1. $K^-\pi^+\pi^+$ mass plots for event samples isolated with the stand-alone vertexing method: a) events with a reconstructed vertex of 3 linked tracks with net charge of ± 1 and at least one track not associated with the same vertex; K mass is assigned to the opposite sign track; b) events from plot a) with compatible Čerenkov identification; c) events from plot a) with a reconstructed primary vertex in the target region; d) requirements b) and c) are both satisfied; e) D^+ candidate tracks from plot d) point back to the primary vertex within $60\mu\text{m}$; f) events with requirements of plot e) but without Čerenkov identification.

Additional cuts on helicity angles, minimum energy, etc. may also be imposed to improve the signal-to-background ratio. Finally, a cut is made on the significance of vertex separation L/σ_L , where L is the distance between secondary and primary vertex and σ_L is the error on that separation. Details of cuts vary with the decay channel under study, but the basic approach remains unchanged. Fig. 2 shows the D^+ signal obtained with a candidate-driven vertex finder for several L/σ_L cuts. As expected, signal size decreases and signal-to-noise ratio improves as the L/σ_L cut increases. Comparison of Figs. 1 and 2 shows that larger signals may be obtained with the candidate-driven approach, but a cleaner sample may be obtained by the stand-alone approach without requiring a large vertex separation cut.

The success of the algorithms in selecting rarer decays is illustrated in Figs. 3 and 4. Fig. 3 shows preliminary results obtained with the stand-alone algorithm. Both D_s^+ and Cabibbo-suppressed D^+ signals are clearly seen in Fig. 3a). In Fig. 3b) is seen the difficulty to isolate Cabibbo-suppressed $D^0 \rightarrow \pi^+\pi^-\pi^+\pi^-$ decay mode. Fig. 4 shows samples isolated with the candidate-driven approach. Figs. 4a) and b) show samples of D_s^+ and D^+ decays to $\phi\pi^+$ from a subsample of the original data containing

about 100,000 $\phi \rightarrow K^+K^-$ decays; Fig. 4c) shows $D^0 \rightarrow K_S^0 K^+ K^-$ decays obtained starting with a subsample containing about 10^6 $K_S^0 \rightarrow \pi^+\pi^-$ decays. E687 is fortunate to have two such highly successful complementary charm selection methods available.

LIFETIMES

Preliminary lifetime values for D^+ and D^0 mesons have been determined for event samples obtained by both techniques using binned maximum likelihood fits with a variety of background and efficiency parameterizations. More details are given in Ref. [3]. Preliminary lifetimes for $D^+ \rightarrow K^-\pi^+\pi^+$ decays of $(1.061 \pm 0.039 \pm 0.020)\text{ps}$ and $(1.092_{-0.018}^{+0.056})\text{ps}$ and for $D^0 \rightarrow K^-\pi^+$ and $D^0 \rightarrow K^-\pi^+\pi^+\pi^-$ decays of $(0.432 \pm 0.016 \pm 0.020)\text{ps}$ and $(0.461 \pm 0.014)\text{ps}$ have been found for samples from candidate-driven algorithms (stat. and syst. errors) and stand-alone algorithms (stat. errors only), respectively. These preliminary lifetime values are all in reasonable agreement with current world averages[7].

Lifetimes for D_s^+ decaying to $\phi\pi^+$ and Λ_c^+ decaying to $pK^-\pi^+$ have also been determined using event maximum likelihood fits, with appropriate background and efficiency parameterizations, to proper time distributions for event samples obtained

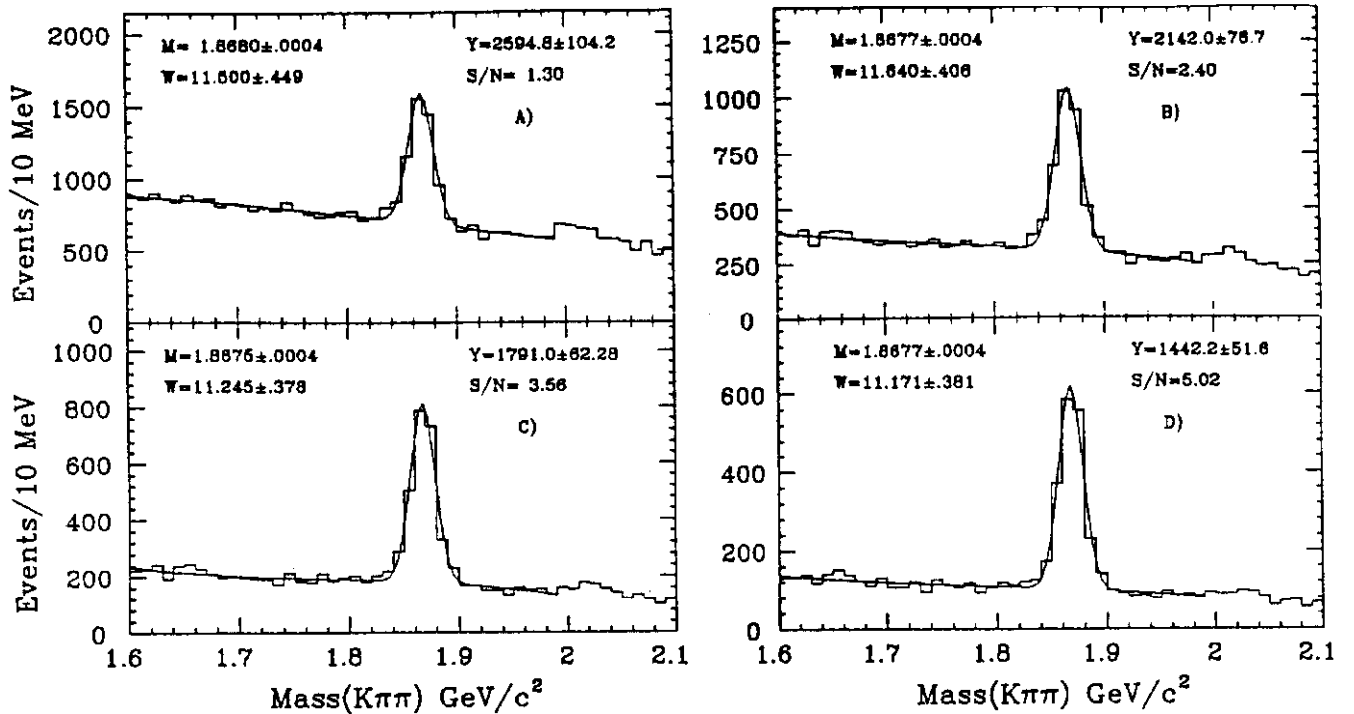


Fig. 2. $K^- \pi^+ \pi^+$ mass plots for event samples isolated using a candidate-driven vertex finder for several L/σ_L cuts: a) $L/\sigma_L > 5$; b) $L/\sigma_L > 8$; c) $L/\sigma_L > 11$; d) $L/\sigma_L > 11$.

by the candidate-driven approach. Preliminary values were reported at this conference [5]. Final lifetime values of $(0.50 \pm 0.06 \pm 0.03)$ ps for the D_s^+ and $(0.20 \pm 0.03 \pm 0.03)$ ps for the Λ_c^+ are given in a paper accepted for publication in Phys. Lett. B [8]. In both cases the values are consistent with current world averages [7], but will continue the trend toward longer lifetimes seen in more recent high-statistics results.

BRANCHING RATIOS

Much remains to be done to improve our knowledge of the many branching ratios and branching fractions for charm particles. E687 will be a source of much information on this subject, but very careful determinations of such factors as Čerenkov identification efficiencies are needed before final values can be given. Here we report on preliminary branching ratio values from work in progress.

Analysis of samples (stand-alone algorithm) of rare Cabibbo-suppressed $D^0 \rightarrow \pi^+ \pi^- \pi^+ \pi^-$ decays (Fig. 3b) and of $D^0 \rightarrow K^- \pi^+ \pi^+ \pi^-$ decays yields the preliminary value of 0.091 ± 0.020 for the ratio $B(D^0 \rightarrow \pi^+ \pi^- \pi^+ \pi^-) / B(D^0 \rightarrow K^- \pi^+ \pi^+ \pi^-)$. An independent analysis of samples from a candidate-driven algorithm yields a preliminary value of 0.114 ± 0.030 for the same branching ratio. Combining both estimates we obtain a preliminary estimate of $B(D^0 \rightarrow \pi^+ \pi^- \pi^+ \pi^-) / B(D^0 \rightarrow K^- \pi^+ \pi^+ \pi^-) = 0.10 \pm$

0.02 ± 0.02 where we have estimated the systematic error to be 2%. This may be compared with the current world average of about 0.045 ± 0.018 estimated from values in Ref. [7].

Preliminary results on $D^0 \rightarrow K_S^0 K^+ K^-$ and $D^0 \rightarrow K_S^0 \pi^+ \pi^-$ decays are also available. Of special interest is the decay $D^0 \rightarrow \bar{K}^0 \phi$ since it can, in principle, serve as a test for the presence of non-spectator decay processes [9]. Fig. 4c) shows a $K_S^0 K^+ K^-$ mass plot obtained using a candidate-driven algorithm. Since $D^0 \rightarrow K_S^0 \pi^+ \pi^-$ decays are more plentiful, tighter cuts can be put on that sample (not shown) which is used as the reference. Fitted signals are weighted as a function of D^0 momentum by the inverses of overall acceptance functions determined from Monte Carlo and other experimental studies. (See Ref. [5].) The preliminary value (stat. errors only) for the inclusive branching ratio is:

$$\frac{B(D^0 \rightarrow \bar{K}^0 K^+ K^-)}{B(D^0 \rightarrow \bar{K}^0 \pi^+ \pi^-)} = \frac{N(D^0 \rightarrow K_S^0 K^+ K^-)}{N(D^0 \rightarrow K_S^0 \pi^+ \pi^-)} = 0.20 \pm 0.06$$

The world average calculated from branching fractions in Ref. [7] is about 0.22 ± 0.05 .

The D^0 can be seen clearly in a two-dimensional scatter plot of $K^+ K^-$ mass as a function of $K_S^0 K^+ K^-$ mass for the $K_S^0 K^+ K^-$ sample. A ϕ mass band and large ϕ peak are obvious at about $1020 \text{ MeV}/c^2$ in the scatter plot and in the corresponding $K^+ K^-$ mass

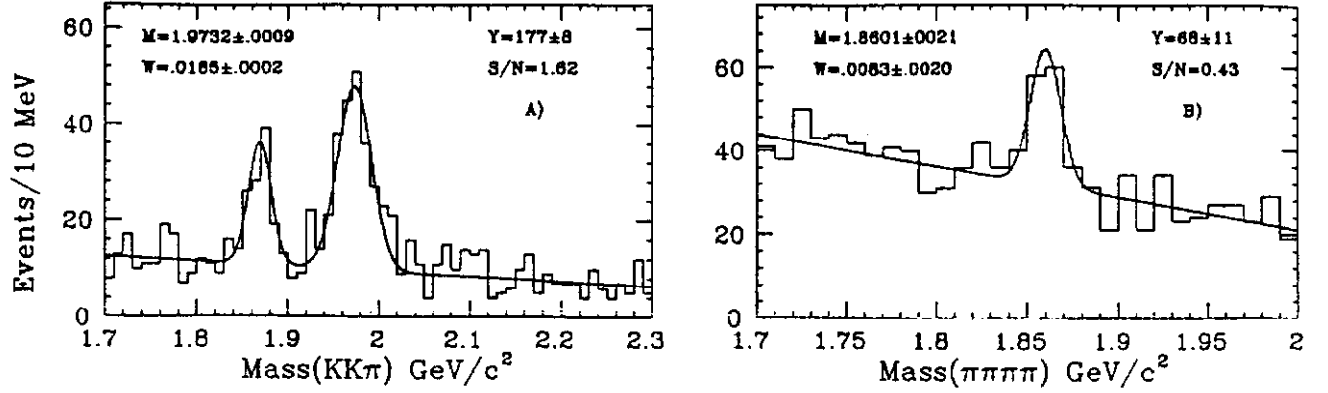


Fig. 3. Mass plots for rare charm decays obtained with the stand-alone algorithm: a) $K^+K^-\pi^+$ mass combinations; b) $\pi^+\pi^-\pi^+\pi^-$ mass combinations.

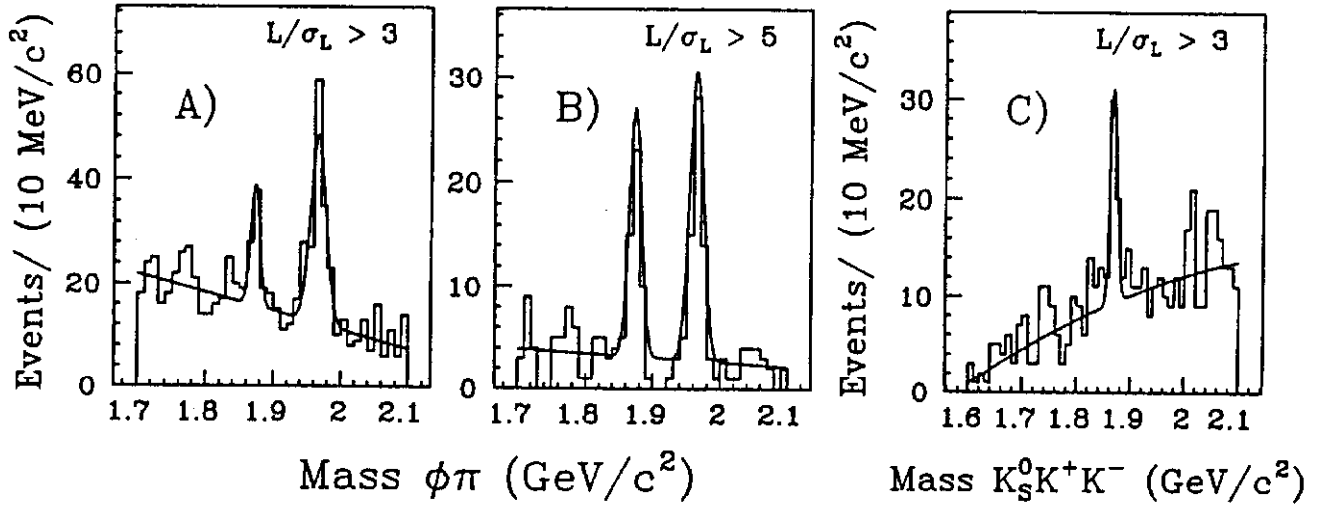


Fig. 4. Mass plots for rare charm decays isolated with the candidate-driven approach: a) and b) $\phi\pi^+$ mass combinations for $L/\sigma_L > 3$ and $L/\sigma_L > 5$, respectively; c). $K_S^0K^+K^-$ combinations for $L/\sigma_L > 3$.

plot. There appears to be an enhancement where the bands overlap on the scatter plot (See Ref. [5]). To determine the fraction of $D^0 \rightarrow K_S^0K^+K^-$ decays via $D^0 \rightarrow K_S^0\phi$, we selected $K_S^0K^+K^-$ events with K^+K^- mass in a ϕ band, $1.010 < M(K^+K^-) < 1.030 \text{ GeV}/c^2$, and determined the D^0 signals in the resulting unweighted and weighted $K_S^0K^+K^-$ mass distributions; D^0 signals in sidebands, if present, are much smaller. The weighted D^0 signal corrected for $B(\phi \rightarrow K^+K^-)$ is used to estimate the branching ratio (statistical error only):

$$\frac{B(D^0 \rightarrow \bar{K}^0\phi)}{B(D^0 \rightarrow \bar{K}^0\pi^+\pi^-)} = 0.16 \pm 0.06$$

This preliminary value is consistent with the ARGUS result [10] of 0.155 ± 0.033 . Fits to Dalitz plots for $D^0 \rightarrow K_S^0K^+K^-$ and $D^0 \rightarrow K_S^0\pi^+\pi^-$ samples will provide better estimates of $\bar{K}^0\phi$, $\bar{K}^0a_0(980)$ and non-resonant $\bar{K}^0K^+K^-$ contributions to the $D^0 \rightarrow \bar{K}^0K^+K^-$ channel and $K^-\pi^+$, $\bar{K}^0\rho^0$ and non-resonant $\bar{K}^0\pi^+\pi^-$ contributions to the $D^0 \rightarrow \bar{K}^0\pi^+\pi^-$ channel.

TOTAL CROSS SECTIONS

Preliminary measurements have been made of photoproduction cross-sections for $D^{*\pm}$ and D^\pm from two independent analyses of D^{*+} photoproduction. The first analysis relied heavily on kinematics. For $D^{*+} \rightarrow D^0\pi^+$, Q-value about 6 MeV, one can cut on the mass difference ΔM and look for a low momentum π to find the clean decay channel $D^{*+} \rightarrow D^0\pi^+$; $D^0 \rightarrow K^-\pi^+$ [11]. This kinematic technique, using a restricted input data sample, yielded a raw sample of 293 ± 32 events. An alternate technique used both the ΔM cut and finite lifetime cuts with a candidate driven vertex algorithm [3]. This technique gave raw samples of 1154 ± 49 $D^{*+} \rightarrow D^0\pi^+$; $D^0 \rightarrow K^-\pi^+$ and $D^0 \rightarrow K^-\pi^+\pi^+\pi^-$ events as well as 1757 ± 70 $D^+ \rightarrow K^-\pi^+\pi^+$ and 5379 ± 248 $D^0 \rightarrow K^-\pi^+$ and $D^0 \rightarrow K^-\pi^+\pi^+\pi^-$ decays. The two D^{*+} analyses are complementary and provide a consistency check.

The fraction of D^0 from the D^{*+} decay chain is 0.237 ± 0.013 , in reasonable agreement with a simple model which predicts 0.29 ± 0.02 with the as-

assumption that D^- 's and D^+ 's are produced in proportion to the number of spin states available (3:1) [12]. The D^- sample can be split according to charge as originating from D^{*+} or D^{*-} decays. The ratio of antiparticle to particle is split evenly within statistics (1.06 ± 0.08), providing no evidence for associated production of meson-baryon states at these energies.

The cross section is obtained from the luminosity (including number of photons on the Be target, targeting efficiency, and live time for data acquisition), the spectrometer acceptance, and the reconstruction and analysis program efficiencies. We also used the D^- to $K\pi\pi$ branching ratio from Ref. [7] to calculate the D^{*+} cross-section.

In the lifetime technique analysis, the uncertainty in incident photon energy ($\approx \pm 45$ GeV) is corrected by de-convoluting the cross section in measured x_F and E_γ bins with the expected energy resolution from Monte Carlo simulation.

The total open charm photoproduction cross section can be derived from the D^{*+} cross section. The ratio of D^{*+} to all photoproduced open charm particles from $c\bar{c}$ is only dependent on charm quark fragmentation after the $c\bar{c}$ pair is created. Using the LUND Monte Carlo program [14][15] with "string fragmentation" we estimate the probability that a

D^{*+} or D^{*-} is produced from a $c\bar{c}$ event to be 0.604. For A dependence of the cross-section, we assumed A^α with $\alpha = 0.93$ following E691's choice [12]. This leads to a total open charm photoproduction cross-section per nucleon of:

$$\sigma_{c\bar{c}}/\text{nucleon} = \frac{\sigma_{D^{*+}}/\text{Be nucleus}}{0.604 \times 9.01^{0.93}}.$$

Raw numbers of events from the lifetime technique must be further corrected for the limited x_F range (this was $x_F > 0.2$ for the D^{*+} and $x_F > 0.0$ for the D^+). We used the E691 parameterization [12] to correct for limited x_F acceptance. The energy dependence of the total open charm cross-section calculated from the two techniques of analyzing the D^{*+} and the lifetime technique for the D^+ is shown in Fig. 5. Also shown is published data from other charm photoproduction experiments. E691 data [12] were multiplied by $1/A^{0.93} = 0.129$ to convert cross section per Be nucleus to per nucleon.

Several parameters must be chosen to compare these results with photon-gluon fusion (PGF) model predictions. The charm quark mass m_c , the QCD scale parameter Λ , the momentum transfer Q^2 , and the gluon distribution $G(x)$ are required. A prediction from the (PGF) [13] using $Q^2 = 10$ GeV² and $\Lambda = 260$ MeV and a naive gluon distribution did not compare well with data. A higher order QCD

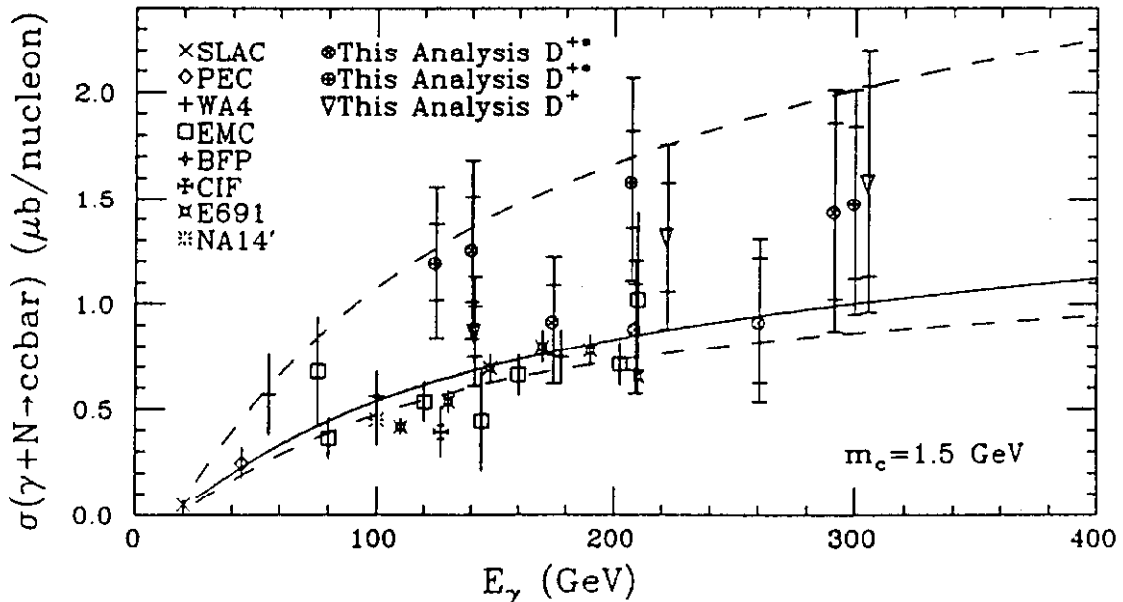


Fig. 5. Photon energy dependence of the total cross-section per nucleon for photoproduction of open charm events. Data points with \otimes are derived from the D^{*+} with the kinematic analysis, \oplus from the D^{*+} and ∇ from the D^+ with the lifetime analysis. For these the inner error is statistical, and the outer error includes the systematic error in quadrature. For the data from CIF, BFP, WA4, SLAC, EMC and PEC see the references listed in [17], for E691 see Ref. [12], and for NA14' see Ref. [18]. The curves are for total charm photoproduction cross-sections with QCD radiative correction assuming a charm mass of $m_c = 1.5$ GeV. [16]. The solid curve is for $\Lambda = 260$ MeV, and the dotted curves are for the uncertainties in Λ and Q^2 .

radiative correction model [16] with $Q^2 = 10 \text{ GeV}^2$, $\Lambda = (260 \pm 100) \text{ MeV}$, $m_c = 1.5 \text{ GeV}$ and a naive gluon distribution is shown in Fig. 5. The dotted curves correspond to variations of $\pm 100 \text{ MeV}$ in Λ and a factor of two in Q^2 . Although this is not a fit to the parameters, the total open charm photoproduction cross-section presented here is in reasonable agreement with other data and the prediction with $m_c = 1.5 \text{ GeV}$.

The p_T^2 dependence of the cross section with acceptance correction was calculated; the resultant differential cross sections $d\sigma/dp_T^2$ for D^{*+} and D^+ are fitted by the empirical form

$$d\sigma/dp_T^2 \propto \exp(-bp_T^2 + cp_T^4),$$

with $b = 1.14 \pm 0.23$ (0.92 ± 0.05) and $c = 0.098 \pm 0.045$ (0.036 ± 0.007) for the $D^{*+}(D^+)$. The average p_T^2 for $D^{*+}(D^+)$ derived from the differential cross-section data is $\langle p_T^2 \rangle = 1.33 \pm 0.68$ (1.26 ± 0.19) GeV^2/c^2 , consistent with the values $1.27 \pm 0.13 \text{ GeV}^2/c^2$ for D^{*+} and $1.21 \pm 0.06 \text{ GeV}^2/c^2$ for D^+ observed by E691 [12].

ACKNOWLEDGEMENTS

We wish to acknowledge the assistance of the staffs of Fermilab, INFN of Italy and the physics departments of the University of Colorado, University of Illinois, Northwestern University, and Notre Dame University. This research was supported in part by the National Science Foundation, the U.S. Department of Energy, the Italian Istituto Nazionale di Fisica Nucleare and Ministero della Universita' e della Ricerca Scientifica.

REFERENCES

- [1] "Photoproduction of D Mesons", FERMILAB-FN-90/555, Paper 702 submitted by D. Buchholz.
- [2] "Description of the E687 Spectrometer", FERMILAB-FN-90/553, Paper 677 submitted by S. Gourlay.
- [3] " D^+ , D^0 Signals and Lifetimes in E687 Photoproduction Experiment at Fermilab", FERMILAB-FN-90/556, Paper 381 submitted by L. Moroni.
- [4] "Measurement of the J/Ψ Elastic Photoproduction from 100 GeV to 400 GeV in the experiment E687 at Fermilab", FERMILAB-FN-90/554, Paper 563 submitted by S.P. Ratti.
- [5] "Some Lifetimes and Branching Ratios for Charmed Hadrons Produced in the Fermilab Wide-Band Photon Beam", FERMILAB-FN-90/557, Paper 589 submitted by W. D. Shephard.
- [6] P.L. Frabetti *et al.*, "Description and Performance of the E687 Spectrometer", to be submitted to Nuclear Instruments and Methods.
- [7] Particle Data Group, Phys. Lett. B239 (1990).
- [8] P.L. Frabetti *et al.*, "Measurement of the D_s^+ and Λ_c^+ Lifetimes", accepted for Publication in Phys. Lett B (1990); also FERMILAB-Pub-90/158-E [E687].
- [9] I.I. Bigi and M. Fukugita, Phys. Lett. B91, 121 (1980).
- [10] H. Albrecht *et al.*, Phys. Lett. B158, 525 (1985).
- [11] S. Park, Ph.D. Thesis, Northwestern University, unpublished (1990).
- [12] J.C. Anjos *et al.*, Phys. Rev. Lett. 62 (1989) 513.
- [13] L.M. Jones and H.W. Wyld, Phys. Rev. D17 (1978) 759.
- [14] G. Ingelman and A. Weigend, "LUCIFER — A Monte Carlo for High- p_{\perp} Photoproduction," Comput. Phys. Commun. 46 (1987) 241.
- [15] T. Sjöstrand and M. Bengtsson, "The Lund Monte Carlo for Jet Fragmentation and e^+e^- Physics — JETSET version 6.3," Comput. Phys. Commun. 39 (1986) 347.
- [16] R.K. Ellis and P. Nason, Nucl. Phys. B312 (1989) 551.
- [17] M.I. Adamovich *et al.*, Photon Emulsion Collab., Phys. Lett. B187 (1987) 437.
- [18] M.P. Alvarez *et al.*, The NA14' Collab., CERN-EP/88-148 (Oct. 1988).